NGL-05-007-009

JR-242

A PERTURBATION PROCEDURE FOR CALCULATING THE EFFECTS

OF LATERAL INHOMOGENEITIES ON THE EARTH'S FREE OSCILLATIONS

*This appendix is Chapter 6 from a Thesis by J. R. McGinley, Jr. and has been slightly modified to be self-contained. Pagination is from the Thesis.

FACILITY FORM 602

N70-77749	
(ACCESSION NUMBER)	(THRU)
37	none
(PAGES)	(CODE)
CR-110819	
(NASA CR OR TMX OR AD NUMBER)	(CATEGORY)

A PERTURBATION PROCEDURE FOR CALCULATING THE EFFECTS OF LATERAL INHOMOGENEITIES ON THE EARTH'S FREE OSCILLATIONS

Notation

$^{\circ}$	this superscript identifies a quantity as appropriate to a spherically symmetric earth model which is considered the unperturbed earth model.
n	this subscript represents the mode type, spheroidal or torsional, and the r, θ, and ϕ mode numbers.
ρ	density
λ and μ	Lamé's constants
$\vec{g}$	gravity
$\vec{u}_n$	n'th displacement eigenfunction
ψ_n	change in the gravitational potential for the n'th eigenfunction.
σ_n	the angular frequency squared for the n'th eigenfunction.
γ	the gravitational constant
r, θ, ϕ	conventional spherical coordinates
p, ℓ, m	the r, θ, and ϕ mode numbers respectively
$,j$	layer index; for example, the radial solution function for a spherically symmetric earth model with mode numbers ℓ and p in the jth layer is $u_{\ell p,j}$.

A Perturbation Procedure for Lateral Inhomogeneities

A perturbation technique is applied to the problem of the free oscillations of the earth. The problem is formulated so that the effect on the free oscillations of regional variations in physical properties can be calculated. This result is related to surface wave dispersion through the implied great circular travel times. The problem is of interest independent of the question of the existence of weak zones in the earth since known differences in dispersion over continental, oceanic, and tectonic regions imply significant lateral differences. Backus (1964) has given a procedure for inverting great circular and great semi-circular phase velocity data for periods when a traveling wave view is appropriate. Toksöz and Anderson (1966) have interpreted observed phase velocity differences over different paths using path-averaging. Smith (1966) has presented free oscillation data showing different observed periods at different stations. The observed differences are probably due to regional variations in earth structure. The theory given here can aid in more precise interpretation of observed differences in free oscillation periods and in connecting free oscillation calculations with the traveling wave viewpoint. Backus and Gilbert (1961) calculated the rotational splitting of the free oscillations of the earth using a perturbation approach. The technique used here is essentially the same although the emphasis is upon an operator formalism which is convenient for lateral variations which occur over a distance which is short compared to the wave length considered.

Two types of perturbations are treated:

a) perturbations in λ and μ for a spherical, gravitating earth model;

b) perturbations in λ, μ, and ρ for a spherical, non-gravitating earth model.

The theory given allows calculation of the first order change in eigenfrequency, as would Rayleigh's principal, and also contains expressions for changes in the eigenfunction and expressions for higher order changes can be formed by simple extensions. The computational effort to obtain more than the first order change in eigenfrequency may be considerable.

For a complete treatment of the problem it is important to extend the theory to include perturbations in density and shape, and the effect of rotation. As mentioned, Backus and Gilbert (1961) have treated rotation and some aspects of perturbations in density have been considered by Backus (1967). The theory and results developed here should be adequate to give good estimates of the effects of lateral inhomogeneities on fundamental mode torsional eigenfrequencies.

The equations of motion for a spherically symmetric, gravitating earth are

$$\rho^\circ\nabla(\vec{g}^\circ\cdot\vec{u}^\circ_n) - \rho^\circ\vec{g}^\circ(\nabla\cdot\vec{u}^\circ_n) - (\lambda^\circ + 2\mathring{\mu})\ \nabla(\nabla\cdot\vec{u}^\circ_n) + \mu^\circ\nabla\mathrm{x}(\nabla\ \mathrm{x}\ \vec{u}^\circ_n)$$

$$-(\nabla\lambda^\circ)(\nabla\cdot\vec{u}^\circ_n) - (\nabla\mu^\circ)\cdot(\nabla\vec{u}^\circ_n + \vec{u}^\circ_n\nabla) - \rho^\circ\nabla\psi^\circ_n = \sigma^\circ_n\ \rho^\circ\ \vec{u}^\circ_n \tag{6-1a}$$

and

$$-4\pi\gamma\nabla\cdot(\rho^\circ\ \vec{u}^\circ_n) + \nabla\cdot(\nabla\psi^\circ_n) = 0 \tag{6-1b}$$

Notations for equations used in Chapter 6 are given in Appendix 12 when not defined here. In equations (6-1 a, b) λ°, μ°, ρ° and g° are functions of r only. If λ and μ are functions of θ and ϕ also, equations (6-1 a, b) become

$$\rho^\circ\nabla(\vec{g}^\circ\cdot\vec{u}_n) - \rho^\circ\vec{g}^\circ(\nabla\cdot\vec{u}_n)-(\lambda + 2\mu)\nabla(\nabla\cdot\vec{u}_n) + \mu\nabla \times (\nabla \times \vec{u}_n)$$

$$-(\nabla\lambda)(\nabla\cdot\vec{u}_n)-(\nabla\mu)\cdot(\nabla\vec{u}_n + \vec{u}_n\nabla) - \rho^\circ\nabla\psi_n = \sigma_n\rho^\circ\vec{u}_n \qquad (6\text{-}2a)$$

and

$$-4\pi\gamma\nabla\cdot(\rho^\circ\,\vec{u}_n) + \nabla\cdot(\nabla\psi_n) = 0 \qquad (6\text{-}2b).$$

Equations (6-1) are given in Alterman <u>et al</u>, (1959) among others; equations (6-2) are given in Hoskins (1920); both follow Love's derivation (Love, 1911; Chapter 7).

Let the differences in λ and μ which change equations (6-1) to (6-2) be small so that σ_n and $\vec{u}_n$, the eigenvalue and eigenfunction for the perturbed problem, are nearly equal to those of the unperturbed problem. Define the perturbations by

$$\lambda^1(r, \theta, \phi) = \lambda(r, \theta, \phi) - \lambda^\circ(r)$$

$$\mu^1(r, \theta, \phi) = \mu(r, \theta, \phi) - \mu^\circ(r) \quad .$$

Then for notational convenience the following definitions are made

$$
L^\circ \equiv \begin{bmatrix} \rho^\circ\nabla(\vec{g}^\circ\cdot\sim) - \rho^\circ\vec{g}^\circ(\nabla\cdot\sim) - (\lambda^\circ + 2\mu^\circ)\nabla(\nabla\cdot\sim) & -\rho^\circ \\ + \mu^\circ\nabla\mathrm{x}(\nabla\ \mathrm{x}\ \sim) - (\nabla\lambda^\circ)(\nabla\cdot\sim) & \\ - (\nabla\mu^\circ)\cdot(\nabla\sim + \sim\nabla) & \\ & \\ -4\pi\gamma\nabla\cdot(\rho^\circ\sim) & \nabla\cdot\sim \end{bmatrix},
$$

$$
\underline{v^\circ_n} \equiv \begin{bmatrix} \vec{u}^\circ_n \\ \nabla\psi^\circ_n \end{bmatrix},
$$

$$
\underline{u^\circ_n} \equiv \begin{bmatrix} \vec{u}^\circ_n \\ 0 \end{bmatrix},
$$

$$
Q \equiv \begin{bmatrix} -(\lambda^1 + 2\mu^1)\nabla(\nabla\cdot\sim) + \mu^1\nabla x\ (\nabla\ x\ \sim) & 0 \\ -(\nabla\lambda^1)(\nabla\cdot\sim) & \\ -(\nabla\mu^1)\cdot(\nabla\sim + \sim\nabla) & \\ 0 & 0 \end{bmatrix},
$$

$$
\underline{v_n} \equiv \begin{bmatrix} \vec{u}_n \\ \nabla\psi_n \end{bmatrix},
$$

and

$$
\underline{u_n} \equiv \begin{bmatrix} \vec{u}_n \\ 0 \end{bmatrix}.
$$

The matrix operator $L_\circ$ is applied to the column vector $\underline{v}_n^\circ$ by using ordinary rules of matrix multiplication so that equations (6-1a, b) are written

$$L^\circ \underline{v}_n^\circ = \sigma_n^\circ \rho^\circ \underline{u}_n^\circ \tag{6-1c}$$,

and equations (6-2a,b) are written

$$(L^\circ + Q)\underline{v}_n = \sigma_n \rho^\circ \underline{u}_n \tag{6-2c}$$.

A procedure is now followed analogous to that given in Dicke and Wittke (1960), (Chapter 14), or Mathews and Walker (1964), (Chapter 10). Equation (6-2c) is written

$$(L^\circ + \alpha Q)\, \underline{v}_n = \sigma_n \rho^\circ \underline{u}_n \tag{6-2d}$$

where α is an arbitrary parameter which identifies the order of the terms in the assumed expansion

$$\underline{v}_n = \underline{v}_n^\circ + \alpha \underline{v}_n^1 + \alpha^2 \underline{v}_n^2 + \cdots \tag{6-3a}$$

$$\underline{u}_n = \underline{u}_n^\circ + \alpha \underline{u}_n^1 + \alpha^2 \underline{u}_n^2 + \cdots \tag{6-3b}$$

$$\sigma_n = \sigma_n^\circ + \alpha \sigma_n^1 + \alpha^2 \sigma_n^2 + \cdots \tag{6-3c}$$.

The column vectors $\underline{v}_n^i$ and $\underline{u}_n^i$ are defined by

$$v_n^i = \begin{bmatrix} \vec{u}_n^i \\ \\ \nabla \psi_n^i \end{bmatrix}$$

and

$$\underline{u}_n^1 = \begin{bmatrix} \vec{u}_n^1 \\ \\ \\ 0 \end{bmatrix} .$$

Substituting equations (6-3a, b, c) into equation (6-2d) and equating coefficients of the same power of α gives for the zero$\underline{\text{th}}$ power of α

$$L^\circ \underline{v}_n^\circ = \sigma_n^\circ \rho^\circ \underline{u}_n^\circ \qquad (6\text{-}4) ,$$

for the first power of α

$$L^\circ \underline{v}_n^1 + Q \underline{u}_n^1 = \sigma_n^\circ \rho^\circ \underline{u}_n^1 + \sigma_n^1 \rho^\circ \underline{u}_n^\circ \qquad (6\text{-}5) ,$$

etc.

$\vec{u}_n^1$ is expanded in terms of the $\vec{u}_m^\circ$

$$\vec{u}_n^1 = \sum_m a_m \vec{u}_m^\circ \qquad (6\text{-}6)$$

where

$$a_m = (\vec{u}_m^{\circ *} , \vec{u}_n^1) .$$

The inner product is defined by

$$(\vec{u}_m^{\circ *} , \vec{u}_n^1) = \iiint \vec{u}_m^{\circ *} \cdot \vec{u}_n^1 \, \rho^\circ d(\text{vol})$$

and the $\vec{u}_m^\circ$ are normalized so that

$$(\vec{u}_m^{\circ *} , \vec{u}_m^\circ) = 1 .$$

Ottelet (1966) has shown that

$$(\vec{u}_m^{\circ *}\ ,\ \vec{u}_\ell^{\circ}) = \delta_{m\ell} \quad .$$

It is assumed that

$$(\nabla\psi_n^1) = \sum_m a_m \nabla\psi_m^\circ \tag{6-7}$$

The constant a_m in equation (6-7) is the same as the constant a_m in equation (6-6) and there has been no use of an orthogonality condition on the $\nabla\psi_m^\circ$ to obtain equation (6-7). Equation (6-2b) is satisfied by this assumption for all orders of α.

From equations (6-6) and (6-7) there follows

$$\underline{v_n^1} = \sum_m a_m \underline{v_n^\circ} \tag{6-8a}$$

and

$$\underline{u_n^1} = \sum_m a_m \underline{u_n^\circ} \tag{6-8b}$$

Substituting equations (6-8a, b) into equation (6-5) and using equation (6-4)

$$\sum_m \sigma_m^\circ a_m \rho^\circ \underline{u_m^\circ} + Q\,\underline{u_n^\circ} = \sigma_n^\circ \sum_m a_m \rho^\circ \underline{u_m^\circ} + \sigma_n^1 \rho^\circ \underline{u_n^\circ} \tag{6-9}$$

The fact that equation (6-2b) is satisfied for all orders of α results in the second of equations (6-9) being satisfied. The first of equations (6-9) is

$$\sum_m \sigma_m^\circ a_m \rho^\circ \vec{u}_m^\circ + Q_{11} \vec{u}_n^\circ = \sigma_n^\circ \sum_m a_m \rho^\circ \vec{u}_m^\circ + \sigma_n^1 \rho^\circ \vec{u}_n^\circ \qquad (6\text{-}10).$$

Taking the vector inner product of equation (6-10) from the right yields

$$\sigma_\ell^\circ a_\ell + (\vec{u}_\ell^{\circ *}, Q_{11}\vec{u}_n^\circ) = \sigma_n^\circ a_\ell + \sigma_n^1 \delta_{\ell n}$$

where

$$(u_\ell^{\circ *}, Q_{11}\vec{u}_n^\circ) = \iiint \vec{u}_\ell^{\circ *} \cdot (Q_{11} \vec{u}_\ell^\circ) \rho^\circ d(\text{vol}).$$

If $\ell = n$,

$$\sigma_n^1 = (\vec{u}_n^{\circ *}, Q^{11} \vec{u}_n^\circ) \quad , \qquad (6\text{-}11)$$

and if $\ell \neq n$

$$a_\ell = \frac{(\vec{u}_\ell^{\circ *}, Q^{11} \vec{u}_n^\circ)}{\sigma_n^\circ - \sigma_\ell^\circ} \qquad (6\text{-}12)$$

Equation (6-11) gives the first order perturbation in the eigenfrequency of the nth mode and equation (6-12) gives the coefficients for the first order change in the eigenfunctions. Further calculations here will involve only equation (6-11), but a few comments are made on the formalism developed above because of its possible use in other studies.

General application of equation (6-12) will involve considerable calculative effort since the inner products of the spheroidal and toroidal eigenfunctions over limited regions of a sphere are involved;

however, the results contain information about the amplitude of the eigenfunction over a slightly inhomogeneous sphere which should be useful in interpreting observed surface wave characteristics in terms of earth structure. Following Morse and Feshback (1953), (Chapter 9), the above procedure can be extended to include the effects of perturbations in boundary shape. This allows treatment of the effect of the varying elevation of the earth's surface. The above development has assumed non-degenerate eigenfunctions which are sufficient for the work which follows since the actual perturbations calculated are ϕ independent which allows choice of an appropriate zero order set of eigenfunctions by inspection. Treatment of more realistic earth models will require extension of the procedure to account for the degeneracy of the eigenfunctions. This is straightforward using known procedures, for example, in any of the last three references.

A simple modification of the above allows application of the formalism to a non-gravitating sphere including perturbations in the density ρ°. Dropping the terms which contain g°, g, ψ_n°, ψ in equations (6-1) and (6-2) and replacing ρ° by $\rho = \rho^\circ + \alpha\Delta\rho$, equation (6-2c) becomes

$$(L^\circ + \alpha Q)\, \underline{v_n} = \sigma_n(\rho^\circ + \alpha\Delta\rho)\, \underline{u_n} \quad .$$

L° and $\underline{v_n^\circ}$ become

$$
L^\circ \equiv \begin{bmatrix} -(\lambda^\circ + 2\mu^\circ)\nabla(\nabla\cdot\sim) + \mu^\circ\,\nabla x(\nabla\ x \sim) & 0 \\ -(\nabla\lambda^\circ)(\nabla\cdot\sim) - (\nabla\mu^\circ)\cdot(\nabla\sim + \sim\nabla) & \\ 0 & 0 \end{bmatrix}
$$

$$
\underline{v_n^\circ} \equiv \begin{bmatrix} \vec{u}_n^\circ \\ 0 \end{bmatrix} .
$$

The rest of the development is essentially as previously leading to the following expressions in place of equations (6-11) and (6-12)

$$
\sigma_n^1 = (\vec{u}_n^{\circ *}, Q_{11}\vec{u}_n^\circ) - \sigma_n^\circ\ (\vec{u}_n^{\circ *}, \Delta\rho\ \vec{u}_n^\circ) \tag{6-11a}
$$

and

$$
a_m^1 = \frac{(\vec{u}_m^{\circ *}, Q_{11}\vec{u}_n^\circ) - \sigma_n^\circ\ (\vec{u}_m^{\circ *}, \Delta\rho\ \vec{u}_n^\circ)}{\sigma_m^\circ - \sigma_n^\circ} \tag{6-12a}
$$

Application of Perturbation Procedure to Torsional Oscillations

The formalism is now applied to the torsional oscillations of a layered, spherical earth model. Since an exact solution is developed for the radial part of the eigenfunctions the Thomson-Haskell matrix technique can be applied in a manner similar to that for the static solution given in Chapter 2. The matrix relations for the period equation for torsional oscillations of a sphere are given in Gilbert and MacDonald (1960) and are not repeated here. However, the solution function used here is different from that of Gilbert and MacDonald and this solution function with the necessary matrix results is given below and in the last section. A derivation of the solution and a note on the sense in which it can be extended to spheroidal modes are given in the last section.

For the torsional modes of either a gravitating or non-gravitating earth model equation (6-1d) becomes

$$\mu^\circ \nabla \times (\nabla \times \vec{u}^\circ_n) - (\nabla \mu^\circ) \cdot (\nabla \vec{u}^\circ_n + \vec{u}^\circ_n \nabla) = \sigma^\circ_n \rho^\circ \vec{u}^\circ_n \quad .$$

The solution to this equation is of the form

$$\vec{u}^\circ_n = N_{m\ell p} \; u_{\ell p} \; (r) \; \vec{C}_{m\ell} \; (\theta, \phi) \quad .$$

As noted previously the subscript n is used for the mode type and for the three subscripts m, ℓ, and p. The $\vec{C}_{m\ell}$ have been defined in Chapter 2 and the constant $N_{m\ell p}$ is defined below so that

$$\iiint_{\substack{\text{over} \\ \text{sphere}}} \vec{u}_n^{\circ *} \cdot \vec{u}_n^{\circ} \, \rho^\circ \, r^2 \sin\theta \, d\theta \, d\phi = 1 \quad .$$

For the solution in each layer μ° is a constant and $\rho^\circ = \frac{R^\circ}{r^2}$ where R° is a constant. The radial solution function is

$$u_{\ell p}(r) = A\, r^{-\frac{1}{2}} \, 2 \cosh ks + B\, r^{-\frac{1}{2}} \, 2 \sinh ks \qquad (6\text{-}13a)$$

if $(\ell + \frac{1}{2}) > \overline{\omega}$ and

$$u_{\ell p}(r) = A\, r^{-\frac{1}{2}} \, 2 \cos KS + B\, r^{-\frac{1}{2}} \, 2 \sin KS \qquad (6\text{-}13b)$$

if $(\ell + \frac{1}{2}) < \overline{\omega}$.

A and B are arbitrary constants and the following definitions apply

$$\overline{\omega} = \frac{R^\circ}{\mu^\circ} \sigma \qquad (6\text{-}14)$$

$$s = \ell n\, r \qquad (6\text{-}15)$$

$$k = \sqrt{(\ell + \tfrac{1}{2})^2 - \overline{\omega}} \qquad (6\text{-}16a) \quad \text{and}$$

$$K = \sqrt{\overline{\omega} - (\ell + \tfrac{1}{2})^2} \qquad (6\text{-}16b) \quad .$$

For a layered earth model with q layers numbered from 1 through q

$$N_{m\ell p} = \frac{1}{\left\{ \sum_{j=1}^{q} R_j^\circ \int_{r_j}^{r_{j-1}} u_{\ell p,j}^2 \, dr \right\}^{\frac{1}{2}} \left\{ \frac{4\pi}{(2\ell+1)} \frac{(\ell+m)!}{(\ell-m)!} \ell(\ell+1) \right\}^{\frac{1}{2}}} \qquad (6\text{-}17)$$

The detailed from of $\int_{r_j}^{r_{j-1}} u^2{}_{\ell p,j} \, dr$ and the necessary matrix forms are given in the last section.

A perturbation in rigidity within the ith layer is considered where

$$\mu_i^1 = \mu_i - \mu_i^\circ \quad \text{constant for} \quad r_L \leqslant r \leqslant r_u$$

$$\theta_L \leqslant \theta \leqslant \theta_u$$

$$0 \leqslant \phi \leqslant 2\pi$$

and

$\mu_i^1 = \mu_i - \mu_i^\circ = 0$ elsewhere. Results are also given for a perturbation in density of similar geometry but with the magnitude of the perturbation determined by

$$\rho_i^1 = \rho_i - \rho_i^\circ = \frac{(R_i - R_i^\circ)}{r^2}$$

where R_i and R_i° are constants.

If $r_L = r_i$ and $r_u = r_{i-1}$, $\theta_L = 0$ and $\theta_u = \pi$, this perturbation is the same as a change μ_i^1 in the rigidity of the $i^{\underline{th}}$ layer of the sphere (or similarly for a change in density). This case was used as a check on the numerical calculations.

For torsional oscillations and these perturbations the perturbation in the operator, Q, is written

$$Q = Q_v + Q_s$$

where

$$Q_v = \begin{bmatrix} \mu_i^1 \nabla x(\nabla\ x\ \sim) & 0 \\ -2\mu_i^1\ \nabla(\nabla \cdot \sim) & \\ 0 & 0 \end{bmatrix} \quad \text{for} \quad \begin{array}{l} r_L \leqslant r \leqslant r_u \quad , \\ \theta_L \leqslant \theta \leqslant \theta_u \\ 0 \leqslant \phi \leqslant 2\pi \end{array}$$

$$Q_v = 0 \text{ elsewhere} \quad ,$$

$$Q_s = \begin{bmatrix} -(\nabla\mu_i^1)\cdot(\nabla_\sim + \sim\nabla) & 0 \\ 0 & 0 \end{bmatrix}$$

and

$$\nabla\mu_i^1 = \hat{r}\ \mu_i^1\ \{\ \delta(r-r_L) - \delta(r-r_u)\ \}$$

$$+ \hat{\theta}\ \frac{\mu_i^1}{r}\ \{\ \delta(\theta-\theta_L) - \delta(\theta-\theta_u)\ \}$$

Equation (6-11a) is then

$$\sigma_n^1 = (\vec{u}_n^{\circ *}, Q_{11s}\, \vec{u}_n^{\circ}) + (\vec{u}_n^{\circ *}, Q_{11v}\, \vec{u}_n^{\circ}) - \sigma_n^{\circ}\, (\vec{u}_n^{\circ *}, \Delta\rho\, \vec{u}_n^{\circ}) \quad .$$

$$(\vec{u}_n^{\circ *}, Q_v \vec{u}_n^{\circ}) = \frac{\mu_i^1}{\mu_i^{\circ}}\, \sigma_n^{\circ}\, \underline{\overline{R}}_v\, \Theta_v \quad ,$$

$$(\vec{u}_n^{\circ *}, Q_s \vec{u}_n^{\circ}) = \frac{\mu_i^1}{R_i^{\circ}} \left\{ \underline{\overline{R}}_s\, \Theta_v + \underline{\overline{R}}_v\, \Theta_s \right\} \quad , \text{ and}$$

$$\sigma_n^{\circ}\, (\vec{u}_n^{\circ *}, \Delta\rho \vec{u}_n^{\circ}) = \frac{(R_i^{\circ} - R_i)}{R_i}\, \sigma_n^{\circ}\, \underline{\overline{R}}_v\, \Theta_v$$

where

$$\underline{\overline{R}}_v = \frac{R_i^{\circ} \int_{r_L}^{r_u} u^2{}_{\ell p,i}\, dr}{\sum_{j=1}^{k} R_j^{\circ} \int_{r_j}^{r_{j-1}} u^2_{\ell p,j}\, dr} \quad ,$$

$$\Theta_v = \frac{\int_{\theta_L}^{\theta_u} \left[m^2 \left(\frac{P_\ell^m}{\sin\theta} \right)^2 + \left(\frac{\partial P_\ell^m}{\partial \theta} \right)^2 \right] \sin\theta\, d\theta}{\frac{2}{(2\ell+1)}\, \frac{(\ell+m)!}{(\ell-m)!}\, \ell(\ell+1)} \quad ,$$

$$\overline{R}_s = \frac{R_i^\circ \left[t_{\ell p,i} \; u_{\ell p,i} \; r^2 \right]_{r_L}^{r_u}}{\sum_{j=1}^{k} R_j^\circ \int_{r_j}^{r_{j-1}} u_{\ell p,j}^2 \, dr} ,$$

$$\Theta_s = \frac{2 \left[\sin\theta \, \frac{\partial P_\ell^m}{\partial\theta} \; S_\ell^m + m^2 \, P_\ell^m \, T_\ell^m \right]_{\theta_L}^{\theta u}}{\frac{2}{(2\ell+1)} \; \frac{(\ell+m)!}{(\ell-m)!} \; \ell(\ell+1)} ,$$

$$t_{\ell p,i} = \frac{\partial u_{\ell p,i}}{\partial r} - \frac{u_{\ell p,i}}{r} ,$$

$$S_\ell^m = -\frac{\cos\theta}{\sin\theta} \frac{\partial P_\ell^m}{\partial\theta} + m^2 \frac{P_\ell^m}{\sin^2\theta} - \frac{\ell(\ell+1)}{2} P_\ell^m ,$$ and

$$T_\ell^m = \frac{1}{\sin\theta} \frac{\partial P_\ell^m}{\partial\theta} - \frac{\cos\theta}{\sin^2\theta} P_\ell^m .$$

Results of Calculations

The preceding expressions were programmed for an earth model with a perturbation in rigidity and a perturbation in density. The geometry of the perturbed region is shown in Figure 6-1. The calculated change in eigenperiod, ΔT, is compared with

$$\Delta T_{AVE} = \frac{2(\theta_u - \theta_L)}{2\pi} (T_1 - T_o)$$

$T_1 - T_o$ is the change in eigenperiod for a change in rigidity extending from $\theta = 0$ to $\theta = \pi$. ΔT_{AVE} will be the change in eigenperiod if $T_1 - T_o$ is reduced in proportion to the angular distance actually covered by the inhomogeneity. Brune et al (1961) and earlier Jeans (1923) showed that the standing wave pattern of a free oscillation can be viewed as resulting from the interference of two traveling waves traveling in opposite directions around a sphere. For the geometry used here the estimate ΔT_{AVE} is appropriate for a source located at the pole with $m = 0$. In particular, for such a source, physical arguments indicate that ΔT_{AVE} should approach ΔT as the wave length of the associated traveling wave becomes small compared to $2(\theta_u - \theta_L)\ r_o$ where r_o is the radius of the sphere.

The particular perturbation used was a change in rigidity or a change in density in a layer 10 km thick centered at 55 km depth. The mantle model used for the results presented in Figure 6-2 was one of Prof. D. L. Anderson's models based on data from shield areas.

The conclusions drawn are not dependent upon small differences in the starting earth model. In Figure 6-2 for a perturbation from $\theta = 15°$ to $\theta = 90°$ the ratio of the breadth of the inhomogeneous region to the wave length appropriate to the standing wave pattern varies from about 1/2 at $\ell = 2$ to about 4 at $\ell = 20$. At $\ell = 2$ the estimate ΔT_{AVE} is good to about 20% while at $\ell = 20$ it is good to better than 5%. Similarly for a perturbation from $\theta = 75°$ to $\theta = 90°$ the same ratio varies from about 1/12 at $\ell = 2$ to about 9/10 at $\ell = 20$. For this case at $\ell = 2$ the estimate ΔT_{AVE} may be in error by a factor of 3 to 4, at $\ell = 10$ it is good to about 20%, while at $\ell = 20$ it is good to about 10%. Similar considerations for the case where the perturbation varies from $\theta = 45°$ to $\theta = 90°$ give intermediate results. The geometry of the perturbations for these cases is sufficiently simple that the relationship between the free oscillation result and a traveling wave view is easily seen. The change in free oscillation period can be directly interpreted in terms of phase velocity for a great circular path by the formula

$$C = \frac{2\pi r_o}{(\ell + \frac{1}{2})T} .$$

The interpretation for other geometries is more complicated, but the above results should suffice for a test of the compatibility of the hypothesis of a regional weak layer in the upper mantle and observed surface wave dispersion.

To be specific the following discussion is limited to the case of a thin weak layer at about 60 km depth. In Table 6-1 the torsional free oscillation periods for three models are listed for several values of the degree number ℓ. λ is the approximate wave length of traveling waves which would interfere to give the free oscillation. In the column "Model G" are the periods for a 35 layer approximation to a Gutenberg earth model. In the column "Model G3" are the periods for a model which is the same except with the rigidity reduced by a factor of 100 in a 1 km thick layer centered at 60.5 km depth. Column b, the percentage differences between the periods for Models G and G3, shows that a regional weak layer with the properties of Model G3 is easily consistent with the long period data. Observed differences for various great circular paths reported by Toksoz and Anderson (1966) are larger than the differences between Models G and G3 even without assuming that the weak layer of Model G3 is of limited extent.

In the column "Model G4" of Table 6-1 are the periods for a 60 km shell with the same properties as the uppermost 60 km of the Gutenberg Model G and with the lower boundary a free surface. Column c is the percentage difference between the periods for Models G and G4. The differences for the long periods are far larger than observational differences and show the expected unacceptability of a world encircling completely decoupling zone. As the period approaches 50 sec the differences in column c rapidly approach the size of observed differences. This results from the concentration of the energy in the mode above the 60 km level.

The results in Figure 6-2 and Table 6-1 give a basis for estimating the effect of a very thin, very weak regional layer on surface wave dispersion. However, although the rigidity changes for models G3 and G4 are limited to a small region in the model, they are not a small proportion of the original rigidities. To evaluate the effect of this, the ratio of the actual period change to the estimate of the period change from perturbation theory is listed for several models in Table 6-2. The basic model is Model G. The column "Model G1" is based on a model like G, but with the rigidity reduced by one-half in a 1 km thick layer centered at 60.5 km depth. Similarly Model G2 has a rigidity reduction to one-tenth of the original value in the same layer. If the ratio given in Table 6-2 is near 1, the perturbation theory gives a good estimate. This is the case for the models with a rigidity reduction of 50% and 90% in a thin layer. With a rigidity reduction of 99% the perturbation estimate is too low by a factor of 3 at $\ell = 100$ ($T \sim 88$ sec). When the rigidity is reduced to zero the perturbation estimate fails, as would be expected. However, the periods calculated for the shell model, listed for model G4, Table 6-1, can serve as estimates of the period which would be deduced from dispersion in a region with a completely decoupled outer layer which was many wave lengths long.

The above results are now combined to estimate the effect on surface wave dispersion of a very thin, very weak zone of limited lateral extent. Column's b and c, Table 6-1, give the period changes due to an earth encircling weak layer. Reference to Anderson's partial derivative tables (Anderson, 1964) shows that the percentage differences for $\ell = 160$ are about as large as will occur for the model considered here. The percentage change is reduced by the approximate ratio of the length of path containing the weak layer to the total length of path. Then it is increased by the approximate maximum ratio of $\Delta T/\Delta T_{AVE}$ for the appropriate ratio of inhomogeneity dimension to wave length. Table 6-3 lists the calculated percentage changes in period. These can also be interpreted as the percentage changes in phase velocity. For long periods the observational differences for different paths reported by Toksoz and Anderson (1966) are used as a measure of an acceptable variation in period. For shorter periods (about 40 to 80 sec) the variations in typical phase velocities for different regions summarized by Brune (1968) are used. These measures of acceptable variations in period are the maximum allowable since they include known regional structural differences other than a weak layer. The results for model G3, Table 6-3, are large but acceptable by the above criteria. For model G4 with ℓ = 20 results were included for all cases for completeness, but they are obviously inappropriate when the weak layer dimension and the path length are both 500 to 2000 km since dispersion for such a long wave length could not be measured over so short a path. For a weak layer dimension of 1000 km and a path length of 40,000 km a 0.83% change is predicted which, although large, is not outside observed limits. For model G4 with ℓ = 160 the changes again are comparable to observed limits.

The calculated changes in eigenperiod are sharply dependent upon the lateral extent, thickness, depth, and rigidity of the weak layer.

For a weak layer to have an appreciable effect on static tilts and strains, its lateral extent must be at least as great as the source to receiver distance, about 200 to 600 km for the observations considered here. To a first approximation the effect of a weak layer with non-zero rigidity is proportional to its thickness. The static models which showed deviations from the half-space tilts and strains which were large enough to correspond to the observations are essentially equivalent to complete decoupling such as characterized Model G4. The percentage variations for Model G4 are comparable with observed variations without accounting for regional differences other than a weak layer. Since other regional differences are undoubtedly important contributors to the observed phase velocity variations, their combination with a weak layer will tend to conflict with phase velocity observations. Although the calculations are uncertain at approximately the level of the discrepancy, the extreme weakening necessary in the static models appears to make some frequency dependence in the rigidity a necessity. Assuming that a weak layer is due to partial melting, the material may show appreciable rigidity at high frequencies and virtually no rigidity at low frequencies. Some rigidity at $\ell = 160$ ($T \approx 57$ sec) such as in Model G3 results in period variations of 0.5% to 2% which are judged acceptable. Longer wave lengths could measure a lower rigidity, but still be consistent with observed differences because of the longer paths necessary to measure them.

It is concluded that if decoupling is to be significantly involved in explaining the static tilt and strain observations and also be consistent with surface wave dispersion data, the decoupling region must have the following properties:

a) the zone or zones of severe decoupling must be very thin, of the order of 1 km or less; and

b) the effective rigidity of the decoupling zone must show frequency dependence.

TORSIONAL SOLUTION USED AND SENSE IN WHICH IT

CAN BE EXTENDED TO THE SPHEROIDAL SOLUTION

The equations governing the radial part of the solution for a spherically symmetric earth model are given in Alterman et al (1959). For torsional motion the equations are

$$\dot{y}_1 = \frac{y_1}{r} + \frac{1}{\mu} y^2$$

$$\dot{y}_2 = \left[\mu \frac{(\ell^2 + \ell - 2)}{r^2} - \sigma\rho \right] y_1 - \frac{3}{r} y_2$$

where the notation is as in Chapter 6 except the superscript ° has been dropped for convenience; y_1 is for the displacement, y_2 is for the stress, and the dot signifies differentiation with respect to r. With the substitutions

$$R = \rho r^2$$

$$v_1 = r^{\frac{1}{2}} y_1$$

$$v_2 = r^{3/2} y_2$$

and $s = \ell n\ r$

these equations can be written

$$
\begin{bmatrix} \dot{v}_1 \\ \\ \dot{v}_2 \end{bmatrix} = \begin{bmatrix} \frac{3}{2} & \frac{1}{\mu} \\ \\ \mu(\ell^2 + \ell - 2) - R\sigma & -\frac{3}{2} \end{bmatrix} \begin{bmatrix} v_1 \\ \\ v_2 \end{bmatrix}
$$

where v_1 and v_2 are functions of s. If μ and R are assumed constant, these equations become a first order set of simultaneous linear ordinary differential equations with constant coefficients. Such a set can be solved in closed form if the roots to the characteristic equation can be found in closed form. The procedure is well known, for example Hildebrand (1949), Chapter 1, and leads to the result given in Chapter 6.

The results necessary to use this solution in the Thomson-Haskell matrix formalism are in the notation of Chapter 3

$$\varepsilon(s) = \begin{bmatrix} 2\cosh ks & 2\sinh ks \\ \mu(2k\sinh ks - 3\cosh ks) & \mu(2k\cosh ks - 3\sinh ks) \end{bmatrix},$$

$$\varepsilon^{-1}(s) = \frac{1}{4\mu k} \begin{bmatrix} \mu(2k\cosh ks - 3\sinh ks) & -2\sinh ks \\ \mu(-2k\sinh ks + 3\cosh ks) & 2\cosh ks \end{bmatrix},$$

$$a_{11} = \cosh k\,d + \frac{3}{2k} \sinh k\,d \quad ,$$

$$a_{12} = \frac{1}{\mu k} \sinh k\,d \quad ,$$

$$a_{21} = \mu k \left(1 - \frac{9}{4k^2}\right) \sinh k\,d \quad ,$$

and

$$a_{22} = \cosh k\,d - \frac{3}{2k} \sinh k\,d$$

where for the $j^{\underline{th}}$ layer

$$d \equiv d_j = s_j - s_{j-1} = \ell n \frac{r_j}{r_{j-1}} .$$

The substitution

$$K = -\,i\,k$$

gives the other solution form.

For the normalization used in Chapter 6 the following results are needed

$$\int_a^b u_{\ell n}^2 \, \rho r^2 \, dr = 2R \left\{\left[\left\{ A'^2 \, a^{2k} + B'^2 \, b^{-2k} \right\} \left\{ \left(\frac{b}{a}\right)^{2k} - 1 \right\} \left\{ \frac{1}{4k} \right\} + A' \, B' \, \ln \left(\frac{b}{a}\right) \right]\right\} ,$$

$$A' = A + B ,$$

$$B' = A - B ,$$

A and B are the coefficients of equation (6-13a) ,

$$\int_a^b u_{\ell n}^2 \, \rho r^2 \, dr = \frac{R}{2} \left\{\left[\left\{ (\alpha^2 - \beta^2) \cos x - 2\alpha\beta \sin x \right\} \left\{ \frac{\sin y}{K} \right\} + (\alpha^2 + \beta^2) \ln \left(\frac{b}{a}\right) \right]\right\} ,$$

$$x = K \ln\left(\frac{r_{j-1}^2}{ab}\right) \quad ,$$

$$y = K \ln\left(\frac{b}{a}\right) \quad ,$$

$$\alpha = v_1(s_{j-1}) \quad ,$$

$$\beta = \frac{3\alpha}{2K} + \frac{v_2(s_{j-1})}{\mu K} \quad ,$$

the subscript j refers to the $j^{\underline{th}}$ layer and $r_{j-1} \leqslant a \leqslant r_j$ and $r_{j-1} \leqslant b \leqslant r_j$.

It is possible to obtain a similar solution for the equations for spheroidal motion but density must be treated in a special manner. In equations (6-1a, b) let the density when it appears on the left hand side of the equals sign be called ρgravity and the density when it appears on the right hand side of the equation be called ρinertial. Make the following assumptions

$$\rho\text{inertial} = \frac{R}{r^2} \quad ,$$

$$\rho\text{gravity} = \frac{\overline{R}}{r} \quad ,$$

$$\vec{g} = g\hat{r} \quad , \quad \text{and}$$

μ, λ, g, R, and $\overline{R}$ are constants, then the substitutions

$$v_i = r^{n/2} \; y_i \quad ,$$

$$n = 1 \text{ for } i \text{ odd},$$

$$n = 3 \text{ for } i \text{ even},$$

into equations (28) through (33) in Alterman et al (1959) result in an equidimensional set of equations in the variables v_i. This set can be reduced to a set of six simultaneous linear ordinary differential equations with constant coefficients by the charge of variable $s = \ell n \; r$. It can be shown that the resulting equations have a closed form solution. The use of two different variations for density is, of course, only a mathematical artifice. This spheroidal solution was not completed since it does not appear to offer any advantages over existing numerical techniques. The existence of this solution was noted here since the author is not aware of it having been recorded previously.

ℓ	λ km	T sec Model G	T sec Model G3	Difference % b	T sec Model G4	Difference % c
2	20,000	2645.50	2645.88	.014	4755.63	79.76
5	7,280	1081.41	1081.79	.035	1797.48	66.22
10	2,670	621.77	622.32	.088	915.25	47.20
20	1,950	361.07	361.79	.20	465.26	26.36
40	988	202.14	202.90	.38	235.11	16.31
80	497	108.00	108.76	.70	118.36	9.59
160	249	56.19	57.05	1.53	59.64	6.14

Torsional Free Oscillation Periods for Three Models

Table 6-1

Table 6-2

Ratio of Perturbation Estimate of Period Change to Actual Period Change

ℓ	Model G1	Model G2	Model G3	Model G4
2	1.0	1.0	1.1	6200
4	1.0	1.0	1.4	3600
8	1.0	1.1	1.8	1400
20	1.0	1.1	2.0	290
50	1.0	1.1	2.2	66
100	1.0		3.0	28

Weak Layer Dimension km	Total Path Length km	Model G3 $\ell=20$ %	Model G3 $\ell=160$ %	Model G4 $\ell=20$ %	Model G4 $\ell=160$ %
40,000	40,000	.20	1.5	26.	6.1
1,000	40,000	.006	.04	.83	.16
1,000	2,000	.13	.79	16.	3.2
1,000	1,000	.25	1.6	33.	6.3
500	2,000	.10	.44	13.	1.8
500	1,000	.20	.88	26.	3.5
500	500	.40	1.8	53.	7.1

Estimated Effect of a Weak Layer

on Dispersion

Table 6-3

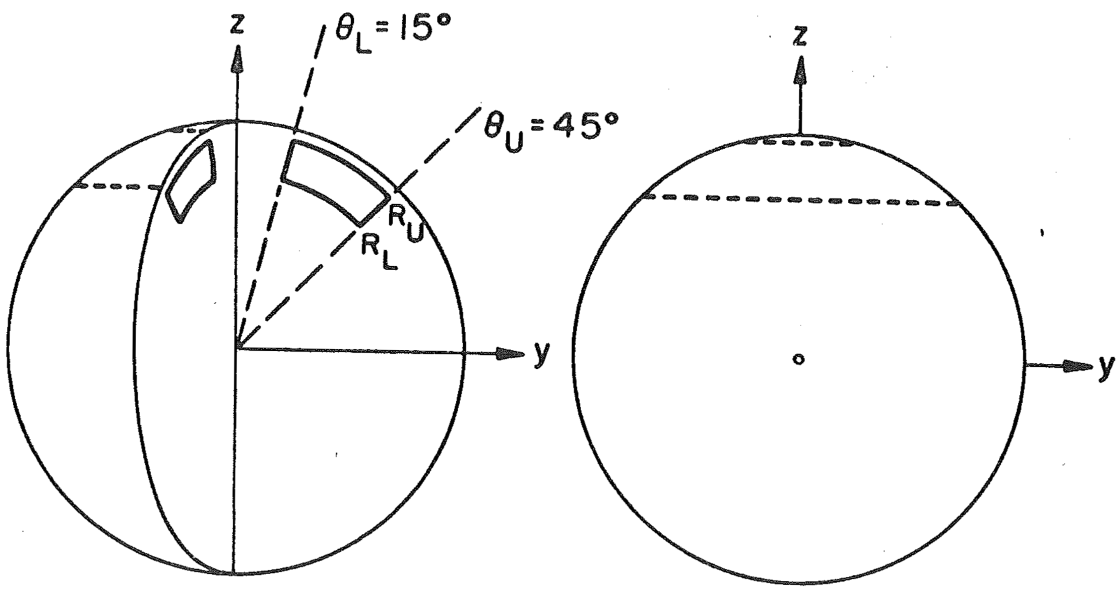

Figure 6-1

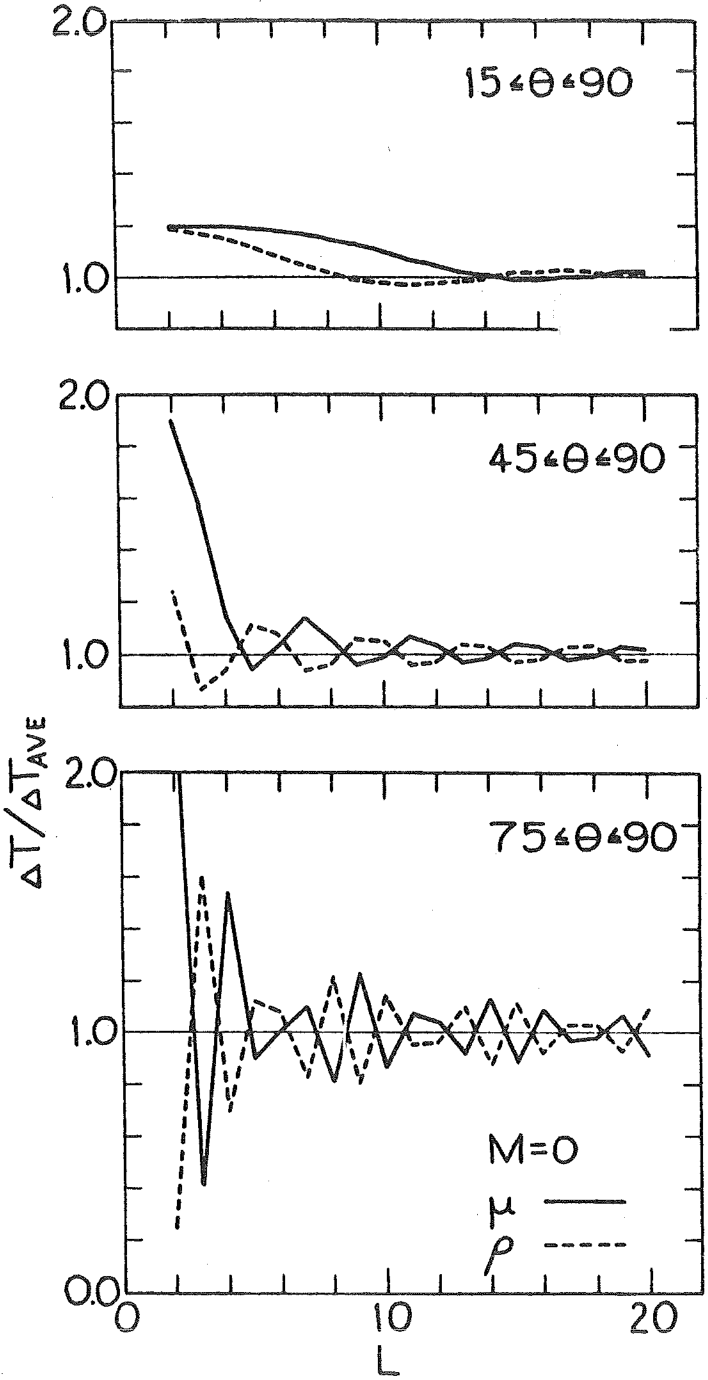

Figure 6-2